

Potential for reversing *miR-634*-mediated cytoprotective processes to improve efficacy of chemotherapy against oral squamous cell carcinoma

Phuong Xuan Tran,^{1,2} Jun Inoue,¹ Hiroyuki Harada,² and Johji Inazawa^{1,3}

¹Department of Molecular Cytogenetics, Medical Research Institute, Tokyo Medical and Dental University (TMDU), Tokyo, Japan; ²Department of Oral and Maxillofacial Surgery, Tokyo Medical and Dental University (TMDU), Tokyo, Japan; ³Bioresource Research Center, Tokyo Medical and Dental University (TMDU), Tokyo, Japan

For advanced oral squamous cell carcinoma (OSCC), increasing sensitivity to chemotherapy is a major challenge in improving treatment outcomes, and targeting cytoprotective processes that lead to the chemotherapy resistance of cancer cells may be therapeutically promising. Tumor-suppressive microRNAs (miRNAs) can target multiple cancer-promoting genes concurrently and are thus expected to be useful seeds for cancer therapeutics. We revealed that *miR-634*-mediated targeting of multiple cytoprotective process-related genes, including cellular inhibitor of apoptosis protein 1 (*cIAP1*), can effectively increase cisplatin (CDDP)-induced cytotoxicity and overcome CDDP resistance in OSCC cells. The combination of topical treatment with *miR-634* ointment and administration of CDDP was synergistically effective against OSCC tumor growth in a xenograft mouse model. Furthermore, the expression of *miR-634* target genes is frequently upregulated in primary OSCC tumors. Our study suggests that reversing *miR-634*-mediated cytoprotective processes activated in cancer cells is a potentially useful strategy to improve CDDP efficacy against advanced OSCC.

INTRODUCTION

Oral cancer is the most frequent malignancy of the head and neck, and over 90% of cases are oral squamous cell carcinoma (OSCC).^{1,2} Although surgical resection and chemoradiation therapy combined with chemodrug and radiation have been developed, they have not been able to clearly improve the prognosis of patients with advanced OSCC.^{3–5} The cis-diamminedichloroplatinum II (cisplatin, CDDP), which is an anticancer agent widely used in chemotherapy against many types of cancers, including OSCC, has cytotoxic effects on cancer cells by inducing apoptotic cell death through DNA damage and oxidative stress.^{5,6} The intrinsic and acquired resistance to CDDP reduces the therapeutic effects of chemotherapy-based treatment.^{5,6} Therefore, improving the sensitivity to CDDP is a major challenge of therapeutic strategies for advanced OSCC.^{5–7} Some cytoprotective processes, including antiapoptotic action, antioxidant effects, and DNA repair, are activated in cancer cells that are resistant to

CDDP, implying that they are a reasonable therapeutic target in increasing CDDP sensitivity.^{5–7}

The inhibitors of apoptosis proteins (IAPs), including X-chromosome-linked IAP (*XIAP*), cellular IAPs (*cIAP1* and *cIAP2*), and *Survivin*, serve as endogenous inhibitors of apoptotic cell death.⁸ IAPs are frequently upregulated in many cancer types, including OSCC, resulting in resistance to cancer treatments.^{8,9} We previously demonstrated that high expression of *cIAP1* via gene amplification at chromosome 11q22 is associated with CDDP resistance and poor patient prognosis in esophageal squamous cell carcinoma (ESCC) and cervical cancers.^{10,11} Furthermore, Debio 1143 (also known as AT-406), a small molecule antagonist of IAPs (*XIAP*, *cIAP1*, and *cIAP2*), was demonstrated to be safe and effective in preclinical models of several cancer types^{12–14} and in combination with chemoradiotherapy for patients with locally advanced head and neck squamous cell carcinoma (HNSCC), including OSCC.^{15–17} Thus, therapeutic targeting of IAPs is a promising approach to improve the efficacy of CDDP-based therapy.

MicroRNAs (miRNAs; miRs), which are functional RNAs consisting of approximately 22 bases, can negatively regulate gene expression by directly binding to the transcripts of multiple target genes.^{18,19} Tumor-suppressive miRNAs (TS-miRNAs) can concurrently target multiple cancer-promoting genes; therefore, miRNA therapeutics using TS-miRNAs as a drug seed are expected to have innovative therapeutic effects.^{19–21} We previously reported that *miR-634* has strong antitumor effects by concurrently targeting multiple cytoprotective

Received 7 November 2021; accepted 11 February 2022;
<https://doi.org/10.1016/j.omto.2022.02.002>

Correspondence: Jun Inoue, PhD, Department of Molecular Cytogenetics, Medical Research Institute, Tokyo Medical and Dental University, 1-5-45 Yushima, Bunkyo-ku, Tokyo 113-8510, Japan.

E-mail: jun.cgen@mri.tmd.ac.jp

Correspondence: Johji Inazawa, MD, PhD, Department of Molecular Cytogenetics, Medical Research Institute, Tokyo Medical and Dental University, 1-5-45 Yushima, Bunkyo-ku, Tokyo 113-8510, Japan.

E-mail: johinaz.cgen@mri.tmd.ac.jp



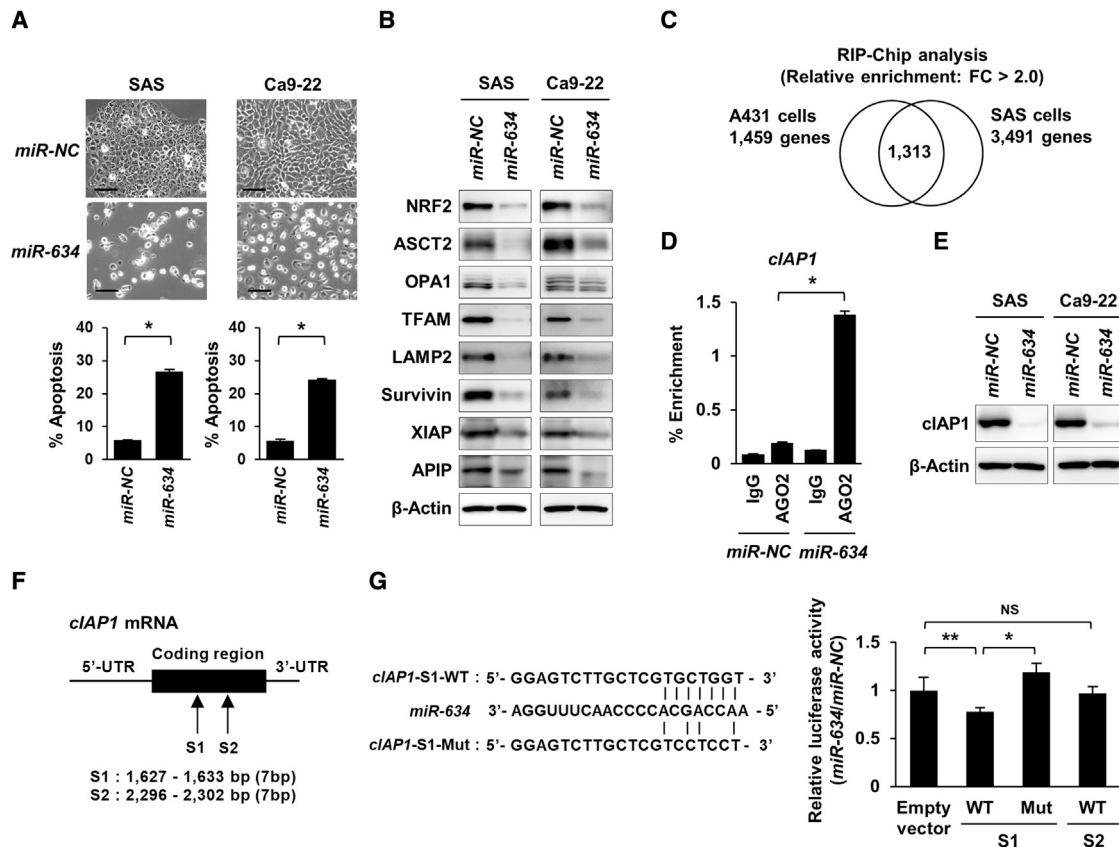


Figure 1. Identification of the *cIAP1* gene as a *miR-634* direct target

(A) Induction of apoptotic cell death by overexpression of *miR-634* in SAS and Ca9-22 cells. Cells were evaluated at day 2 after transfection with 20 nM *miR-NC* or *miR-634*. Upper: phase-contrast images in the miRNA-transfected cells. Scale bars: 20 μ m. Lower: FACS analysis of the apoptotic cell population. (B) Western blot analysis of the miRNA-transfected cells. Cell lysates were prepared two days after transfection. (C) Identification of *miR-634* target genes by RIP-Chip analysis in SAS and A431 cells. In total, 3,491 and 1,459 genes were identified as the candidates with a fold change (FC) > 2.0 by RIP-Chip analysis in SAS and A431 cells, respectively; 1,313 genes identified by both analyses were defined as the *miR-634* target genes. (D) RIP-PCR analysis of the *cIAP1* gene. Enrichment relative to IgG immunoprecipitation in *miR-NC*-transfected cells is presented. (E) Western blot analysis of *cIAP1* in the miRNA-transfected cells. (F) The positions of two putative *miR-634* binding sites (site 1; S1 and site 2; S2) within the coding region of the *cIAP1* gene (accession No. NM_001166; 3,764 bp) are indicated. (G) Luciferase assay using reporter plasmids. Seed sequences of *miR-634* and its mutant sequences are indicated. SAS cells were cotransfected with a reporter plasmid and an internal control vector, and after 5 h, either *miR-NC* or *miR-634* was additionally transfected. Thirty-six hours after transfection, luciferase activity was measured. The luciferase activity in *miR-634*-transfected cells relative to that in *miR-NC*-transfected cells is indicated on the vertical axis. In (A), (D), and (G), error bars indicate the SD of triplicate experiments, and data are presented as the mean \pm SD. *p* values were calculated using the two-sided Student's *t* test (A and D) or one-way ANOVA (G). **p* < 0.0001, ***p* < 0.005. NS, not significant.

process-related genes, including mitochondrial homeostasis (*OPA1* and *TFAM*), antiapoptosis signaling (*APIP*, *XIAP*, and *Survivin*), antioxidant scavenging (*NRF2*), lysosomal degradation (*LAMP2*), and glutaminolysis (*ASCT2*).^{22–24} Furthermore, systemic administration of lipid nanoparticles harboring synthetic *miR-634* mimics suppressed tumor growth in a xenograft mouse model.²⁵ More recently, the topical treatment of an ointment containing synthetic *miR-634* mimics, *miR-634* ointment, was therapeutically effective in a xenograft mouse model of cutaneous squamous cell carcinoma (cSCC) and anaplastic thyroid cancer (ATC).^{24,26} Thus, we demonstrated the practicality of synthetic *miR-634* mimics in miRNA therapeutics. In addition, forced expression of *miR-634* can increase CDDP efficacy in ESCC cells; however, its molecular mechanism remains unclear.²³ In the present study, we investigated the therapeutic potential and

biological significance of *miR-634*-mediated targeting of cytoprotective processes for improving CDDP efficacy against OSCC. Furthermore, we tested the potential of *miR-634* ointment as a topical medication for OSCC that is physically accessible to the tumor.

RESULTS

Identification of the *cIAP1* gene as a *miR-634* target gene

We first found that the forced expression of *miR-634* effectively induces apoptotic cell death in two OSCC cell lines, SAS and Ca9-22, accompanied by the downregulation of eight known target genes for *miR-634*, including *NRF2*, *ASCT2*, *OPA1*, *TFAM*, *LAMP2*, *Survivin*, *XIAP*, and *APIP* (Figures 1A and 1B). To further understand the *miR-634*-mediated tumor-suppressive function, we searched for the target genes of *miR-634* in SAS cells. The RNA-induced silencing

complex (RISC), which consists of a ribonucleoprotein (RNP), such as argonaute 2 (AGO2), can direct the interaction between miRNAs and target mRNAs.^{24,27} To identify mRNAs interacting with RISC, we performed RNP immunoprecipitation (RIP) assays using an antibody against AGO2 in *miR-NC*- or *miR-634*-transfected SAS cells, followed by microarray analysis (RIP-Chip analysis).^{24,28} The enrichment indicated by RIP mRNA levels relative to the total mRNA levels (input) was calculated for *miR-NC*- or *miR-634*-transfected SAS cells.²⁴ As a result, we identified 3,491 target genes, including known *miR-634* target genes, which were enriched by RIP with a greater than 2.0-fold change in *miR-634*-transfected cells relative to *miR-NC*-transfected cells (Figure 1C). In combination with the 1,459 target genes previously identified by the RIP-Chip analysis in A431 cells, a cSCC cell line,²⁴ 1,313 genes were commonly considered as target genes of *miR-634* (Figures 1C and Table S1). Kyoto Encyclopedia of Genes and Genomes (KEGG) pathway analysis revealed that a number of genes related to metabolic pathways were enriched among the identified *miR-634* target genes (Table S2). Among the 1,313 genes, we found *cIAP1*, whose expression is involved in chemotherapeutic resistance, including CDDP (listed as BIRC2 in Table S1; FC:5.22 in A431 cells and FC:10.01 in SAS cells). RIP-PCR analysis revealed the enrichment of *cIAP1* mRNA by RIP with the anti-AGO2 antibody in *miR-634*-transfected SAS cells (Figure 1D). The expression levels of *cIAP1* protein were reduced by overexpression of *miR-634* in SAS and Ca9-22 cells in western blot analysis (Figure 1E). We found two putative *miR-634* binding sites (site 1 [S1] and site 2 [S2]) that are complementary to the *miR-634* seed sequence within the coding region of *cIAP1* mRNA (Figure 1F). The activity of the luciferase vector with the genomic sequences for only S1, not S2, was significantly reduced compared with that of the empty vector, and this reduction was restored by the mutation of a putative binding site for S1 (Figure 1G). Thus, we identified *cIAP1* as a direct target gene of *miR-634*.

Potential of *miR-634* for improving CDDP efficacy against OSCC cells

Next, we examined whether the forced expression of *miR-634* can increase CDDP-induced cytotoxicity in OSCC cells. Two OSCC cell lines, SAS and Ca9-22, were transfected with increasing doses of *miR-634* and simultaneously treated with CDDP. The cell survival rate was reduced by the treatment with a combination of CDDP and *miR-634* at different doses (Figure 2A). The analysis of the combination index (CI) revealed synergistic effects between CDDP and *miR-634* in SAS and Ca9-22 cells (Table S3). We confirmed that the frequency of apoptotic cell death synergistically increased by combined treatment with *miR-634* and CDDP by fluorescence-activated cell sorting (FACS) analysis in both cell lines (Figure 2B). Furthermore, western blot analysis revealed that the levels of cleaved caspase-3 (cCasp-3) and cleaved poly-ADP-ribose polymerase (cPARP) markedly increased in cells treated with the combination, accompanied by the downregulation of target genes (Figure 2C). Additionally, we showed that the intracellular reactive oxygen species (ROS) levels synergistically increased in SAS and Ca9-22 cells treated with the combination (Figure S1). In a previous study, we have demonstrated the synergistic antitumor effect of *miR-634* and CDDP in ESCC.²³

The remarkable synergistic effect by the combination was also shown in two cell lines from other cancer types, T24 (bladder cancer cell line) and A2780 (ovarian cancer cell line) (Figure S2), suggesting that overexpression of *miR-634* may enhance the efficacy of CDDP across various cancer types. Furthermore, a small interfering RNA (siRNA)-mediated knockdown of *cIAP1* or a treatment with AT406, an IAP inhibitor, partially increased CDDP-induced apoptotic cell death in SAS and Ca9-22 cells (Figure 2D). In addition, cPARP levels, but not cCasp-3, were increased by the combination treatment with *cIAP1* knockdown or AT406 and CDDP on western blotting (Figure 2E). Thus, *miR-634*-mediated inhibition of *cIAP1* plays a partial role in the synergistic effects of *miR-634* and CDDP. Moreover, single knockdown of each of the other eight target genes, including *NRF2*, *ASCT2*, *OPA1*, *TFAM*, *LAMP2*, *Survivin*, *XIAP*, and *APIP*, partially increased the frequency of CDDP-induced cell death in SAS and Ca9-22 cells (except for *LAMP2* in SAS cells and *TFAM* in Ca9-22 cells) (Figures 3 and S3). Taken together, these results indicate that concurrent *miR-634*-mediated targeting of multiple cytoprotective process-related genes, including *cIAP1*, is more effective than targeting individual genes separately for improving CDDP efficacy against OSCC cells.

Potential of *miR-634* for overcoming CDDP resistance in OSCC cells

We previously found that overexpression of *miR-634* does not effectively induce cell death in normal human cells, such as fibroblasts.²³⁻²⁵ Consistent with this, *miR-634*-induced cell death did not occur in RT7 cells, an immortalized cell line derived from normal oral epithelial cells (Figure S4).²⁹ Furthermore, we showed that the expression of *miR-634* was markedly downregulated in 6 OSCC cell lines, compared with that of RT7 cells (Figure S5). We next examined the relationship between the CDDP sensitivity, which is defined as the half-maximal inhibitory concentration (IC₅₀), and the expression status of *miR-634* target genes in six OSCC cell lines (HSC-4, HSC-6, SAS, Ca9-22, HOC313, and TSU) and RT7 cells (Figures 4A and S6). As a result, the expression level of *cIAP1* was higher in two CDDP-resistant cells, HOC313 (IC₅₀, >30 μM) and TSU (IC₅₀, 18.4 μM), than in the other CDDP-sensitive OSCC cell lines and RT7 cells (Figure 4A). Of note, we detected *cIAP1* amplification in TSU cells by genomic-PCR analysis (Figure 4B). In addition, *in silico* analysis demonstrated a positive correlation between copy number and expression levels of *cIAP1* in primary HNSCC tumors, including OSCC (Figure 4C). siRNA-mediated knockdown of *cIAP1* alone increased CDDP-induced cytotoxicity in TSU cells, suggesting that activation of *cIAP1* plays a partial role in the CDDP resistance (Figure S7). Importantly, overexpression of *miR-634* synergistically increased the frequency of CDDP-induced apoptotic cell death by FACS analysis in TSU cells, accompanied by increased levels of cCasp-3 and cPARP and the downregulation of *miR-634* target genes, including *cIAP1* (Figures 4D and 4E). We also generated CDDP-acquired resistant cells (Ca9-22-R cells) from Ca9-22 cells (IC₅₀, 13.3 μM in Ca9-22 cells and 32.7 μM in Ca9-22-R cells) (Figure 4F). We confirmed increased sensitivity to CDDP together with the downregulation of *miR-634* target genes, including *cIAP1*, in Ca9-22-R cells (Figures 4G and 4H). Taken

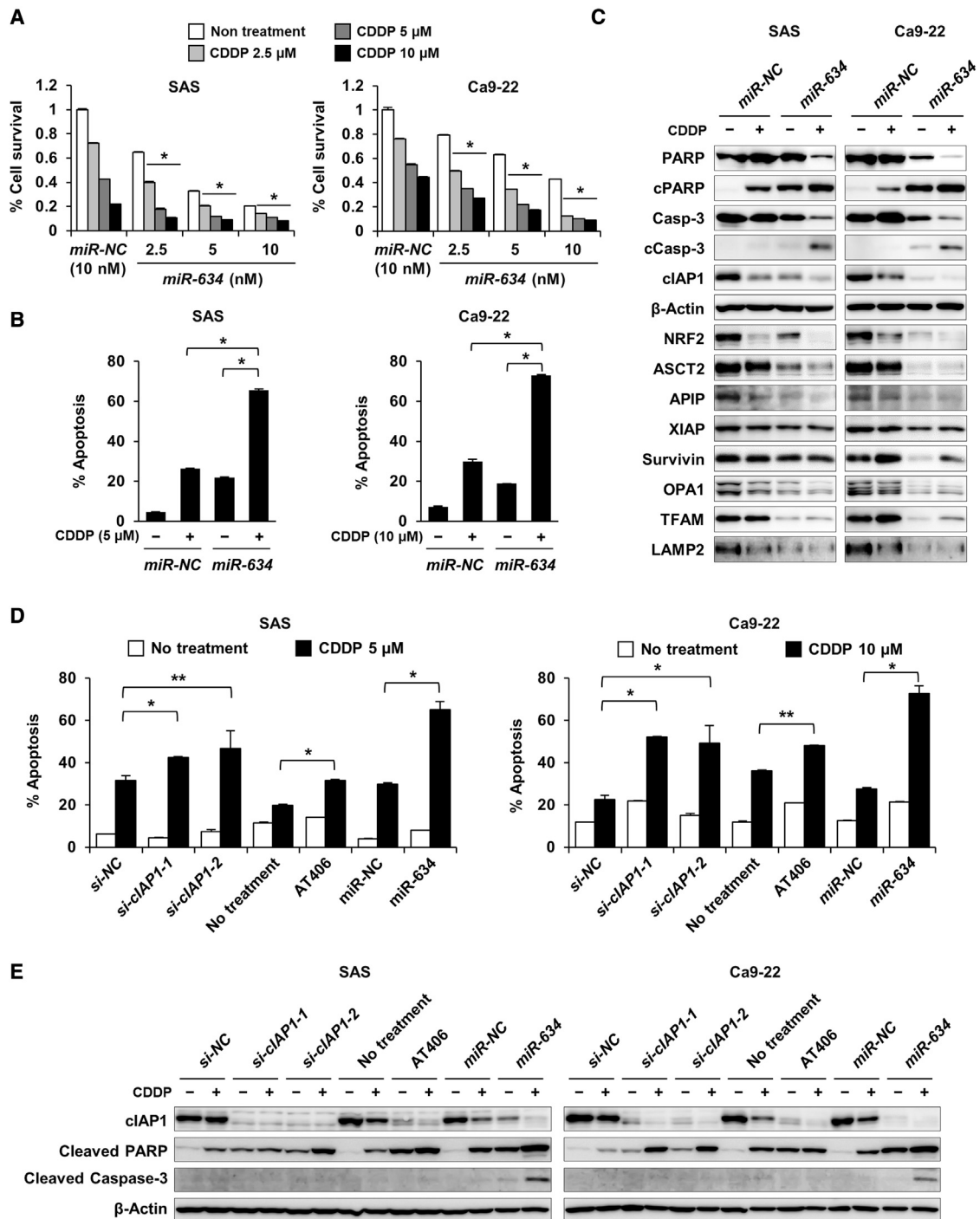


Figure 2. Enhancement of CDDP-induced cytotoxicity by *miR-634* in OSCC cells

(A) Cell survival assay. Cells were transfected with increasing doses of *miR-634* (2.5–10 nM) and treated with CDDP (2.5–10 μ M) for two days from the following day. The results are reported as the relative rate compared with *miR-NC*-transfected and non-treated cells. (B) FACS analysis of the apoptotic cell population among cells with miRNAs and/or CDDP. Cells were transfected with miRNAs (2.5 nM) and treated with CDDP for two days from the following day. (C) Western blot analysis of cleaved caspase-3 (cCasp-3) and cleaved PARP (cPARP) as the apoptosis markers and the *miR-634* target genes. (D) FACS analysis of the apoptotic cell population. Cells were transfected with siRNAs (10 nM) and treated with CDDP for two days from the following day or were concurrently treated with AT406 (10 μ M) and CDDP for two days. (E) Western blot analysis of apoptosis markers and cIAP1. In (A), (B), and (D), error bars indicate the SD of triplicate experiments, and data are presented as the mean \pm SD. p values were calculated using the two-way ANOVA (A and B) and two-sided Student's t test (D). * $p < 0.0001$, ** $p < 0.005$.

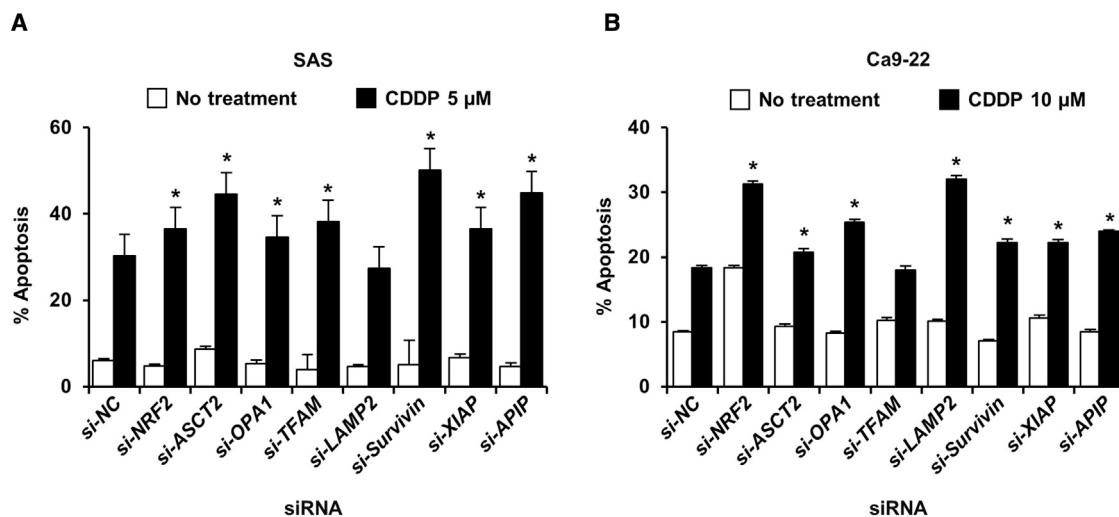


Figure 3. Effects of knockdown of *miR-634* target genes on CDDP-induced cytotoxicity

(A and B) FACS analysis of the apoptotic cell population among SAS cells (A) and Ca9-22 cells (B). Cells were transfected with each siRNA (10 nM) and treated with CDDP for two days from the following day. Error bars indicate the SD of triplicate experiments, and data are presented as the mean \pm SD. p values were calculated using the two-sided Student's t test. *p < 0.0001.

together, these results indicate the forced expression of *miR-634* is a reasonable approach for overcoming intrinsic and acquired resistance to CDDP in OSCC cells.

Synergistic antitumor effects by combination with *miR-634* ointment and CDDP *in vivo*

We next assessed whether the topical treatment of *miR-634* ointment on the tumor can increase CDDP efficacy in xenograft mouse models. *miR-NC* or *miR-634* ointment was topically applied to the subcutaneous tumors every other day (days 4, 6, 8, 10, 12, 14, and 16 after cell injection), and PBS or CDDP was intraperitoneally (IP) administered four times for 12 days (days 4, 8, 12, and 16 after cell injection) (Figure 5A). *In vivo* tumor growth was synergistically inhibited in mice treated with CDDP + *miR-634* ointment compared with mice treated with CDDP + *miR-NC* ointment or PBS + *miR-634* ointment (Figures 5B–5D). qRT-PCR analysis confirmed that the delivery of *miR-634* into xenograft tumor cells is dependent on the size of the tumor (Figure 5E). Furthermore, we confirmed the effective downregulation of *miR-634* target genes, including *cIAP1*, *XIAP*, and *TFAM*, by immunohistochemical analysis in xenograft tumors with *miR-634* ointment (Figure 5F). This suggests that topical treatment with the *miR-634* ointment is a potential therapeutic strategy for improving the efficacy of CDDP in advanced OSCC therapy.

Upregulation of *miR-634* target genes in primary OSCC tumors

Lastly, we examined the expression status of nine *miR-634* target genes in primary HNSCC tumors, including OSCC. The *in silico* analysis using the expression data for 43 paired samples of primary tumors and the corresponding non-tumor tissues revealed that *miR-634* target genes, notably *Survivin*, *ASCT2*, *OPA1*, *cIAP1*, *LAMP2*, and *XIAP*, are significantly upregulated in tumors relative to the cor-

responding non-tumor tissues (Figure 6A). The status with high expression of at least one of the nine genes was observed in 42 of 43 cases (97.7%) (Figure 6B). Furthermore, high expression of *cIAP1* was significantly associated with the recurrence-free survival (RFS) rate based on expression data of 124 cases of HNSCC, including OSCC (Figure 6C). In addition, patients with a high expression of four target genes, including *Survivin*, *OPA1*, *TFAM*, and *LAMP2*, had a shorter overall survival (OS) time (Figure S8). Thus, upregulation of *miR-634* target genes is closely associated with the recurrence and poor prognosis of OSCC patients.

DISCUSSION

Our previous studies revealed that *miR-634* can target multiple cytoprotective process-related genes, including *NRF2*, *ASCT2*, *XIAP*, *APIP*, *Survivin*, *OPA1*, *TFAM*, and *LAMP2*.^{22–24} In the current study, we newly identified the *cIAP1* gene as a target gene of *miR-634*. The IAP family members (*cIAP1*, *XIAP*, and *Survivin*) and *APIP* function as endogenous inhibitors of apoptotic cell death by inhibiting caspase activity and their upregulation leads to chemotherapeutic resistance in cancer cells.^{30,31} Therefore, *miR-634*-mediated targeting of the antiapoptotic process can facilitate CDDP-induced apoptotic cell death. On the other hand, CDDP-induced cytotoxicity is closely associated with oxidative stress via excess accumulation of ROS.³² The transcription factor *NRF2* can attenuate chemodrug-induced ROS production via the activation of genes related to ROS scavenging.³³ The transporter *ASCT2*-mediated glutamine uptake into cancer cells is essential for the generation of intracellular glutathione as an antioxidant.³⁴ Knockdown of *OPA1* and *TFAM*, which are genes related to mitochondrial homeostasis, led to increased ROS production via mitochondrial injury.^{35,36} Furthermore, *LAMP2*, a lysosomal membrane protein, functions in the removal of damaged mitochondria

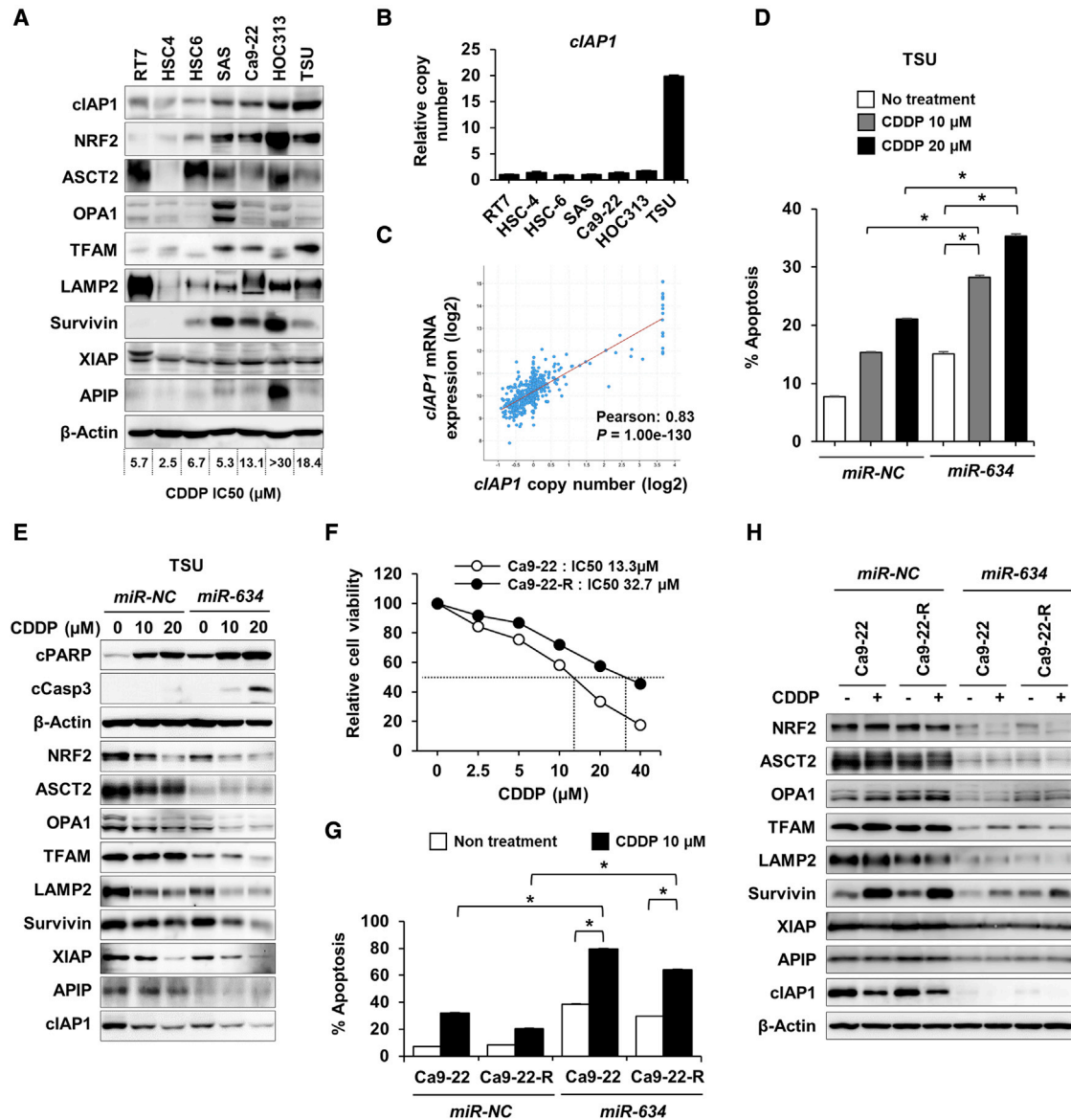


Figure 4. Overcoming CDDP resistance by *miR-634* in OSCC cells

(A) Western blot analysis of *miR-634* target genes in RT7 cells and six OSCC cell lines. IC50 values (μM) for CDDP treatment for each cell line are indicated. (B) Quantitative genomic-PCR for the *cIAP1* gene in OSCC cell lines. The copy number ratios are presented relative to the copy number in RT7 cells. (C) The correlation between copy number and the corresponding mRNA expression of the *cIAP1* gene in 496 cases of HNSCC, including OSCC, from TCGA data. (D) FACS analysis of the apoptotic cell population among TSU cells. Cells were transfected with miRNAs (2.5 nM) and treated with CDDP for two days from the following day. (E) Western blot analysis of cleaved caspase-3 (cCasp-3) and cleaved PARP (cPARP) as the apoptosis markers, and the *miR-634* target genes in TSU cells. (F) Generation of CDDP-acquired resistant cells (Ca9-22-R) from Ca9-22 cells. IC50 values are indicated. (G) FACS analysis of the apoptotic cell population among Ca9-22 and Ca9-22-R cells. Cells were transfected with *miR-634* (2.5 nM) and treated with CDDP (10 μM) for two days from the following day. (H) Western blot analysis of *miR-634* target genes in Ca9-22 and Ca9-22-R cells. In D and G, error bars indicate the SD of triplicate experiments, and data are presented as the mean ± SD. p values were calculated using the two-way ANOVA. *p < 0.0001.

via the autophagy-lysosomal degradation process, and its knockdown results in excess ROS production.³⁷ Importantly, expression of these genes related to antioxidant processes attenuates CDDP sensitivity; therefore, *miR-634*-mediated targeting of the antioxidant processes can increase CDDP-induced cytotoxicity by inducing oxidative stress.

Furthermore, because the expression of the *miR-634* target gene is frequently activated in OSCC tumors, reversing *miR-634*-mediated cytoprotective processes, including antiapoptosis and antioxidant processes, is a reasonable therapeutic strategy to improve CDDP efficacy against advanced OSCC cells.

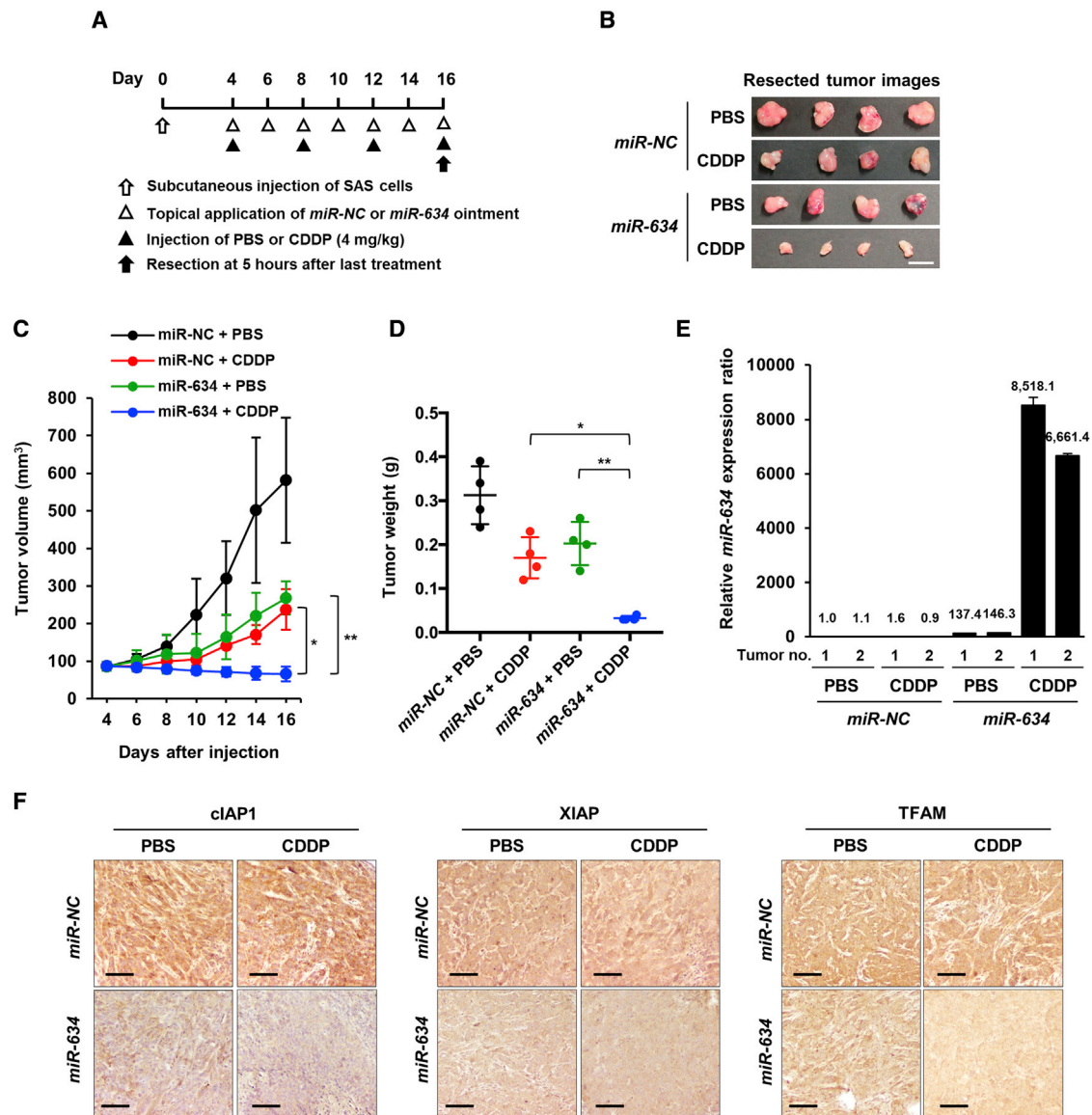


Figure 5. Improvement of the CDDP efficacy by topical application of *miR-634* ointment in SAS xenograft mouse model

(A) Experimental schedule for combined treatment with an ointment and CDDP. (B) Representative images of resected tumors. Scale bar: 1 cm. (C) Tumor volume in mice treated with vehicle + *miR-NC* ointment (n = 4), CDDP + *miR-NC* ointment (n = 4), vehicle + *miR-634* ointment (n = 4), or CDDP + *miR-634* ointment (n = 4). Error bars indicate the SD. Data are presented as the mean ± SD. p values were calculated using two-way ANOVA (*p = 0.0409, **p = 0.0254). (D) The tumor weight in mice treated is presented in the scatterplot. p values were calculated using two-way ANOVA (*p = 0.007, **p = 0.0014). (E) Expression analysis of *miR-634* in resected tumors by qRT-PCR. The expression values are presented relative to the value of tumor with vehicle + *miR-NC* ointment. Error bars indicate the SD of triplicate experiments. Data are presented as the mean ± SD. (F) Immunohistochemical analysis of resected tumors. Scale bars: 50 μm.

We formulated an ointment incorporating synthetic *miR-634* mimics using the ionic liquid transdermal system (ILTS), which improves the transdermal permeability of nucleotides in skin tissue.^{21,24,38,39} In a previous study, we demonstrated rapid permeability and delivery of *miR-634* into tumor cells within 1 h after topical application of an ointment in a xenograft mouse model.²⁴ Additionally, we also found that the forced expression of *miR-634* is not effective in cells of RT7, an immortalized cell line derived

from normal oral epithelial cells, implying the safety of *miR-634* delivery into the normal oral mucosa. Chemoradiation therapy is used to treat patients with advanced OSCC who are unable to undergo surgery due to elderly age or cosmetic reasons or who are administered as adjuvant therapy after surgery.^{3,4,40} In such cases, topical application of *miR-634* ointment may be useful to enhance the therapeutic effects of chemoradiation therapy and to prevent post-surgical recurrence by acting only on residual cancer cells within

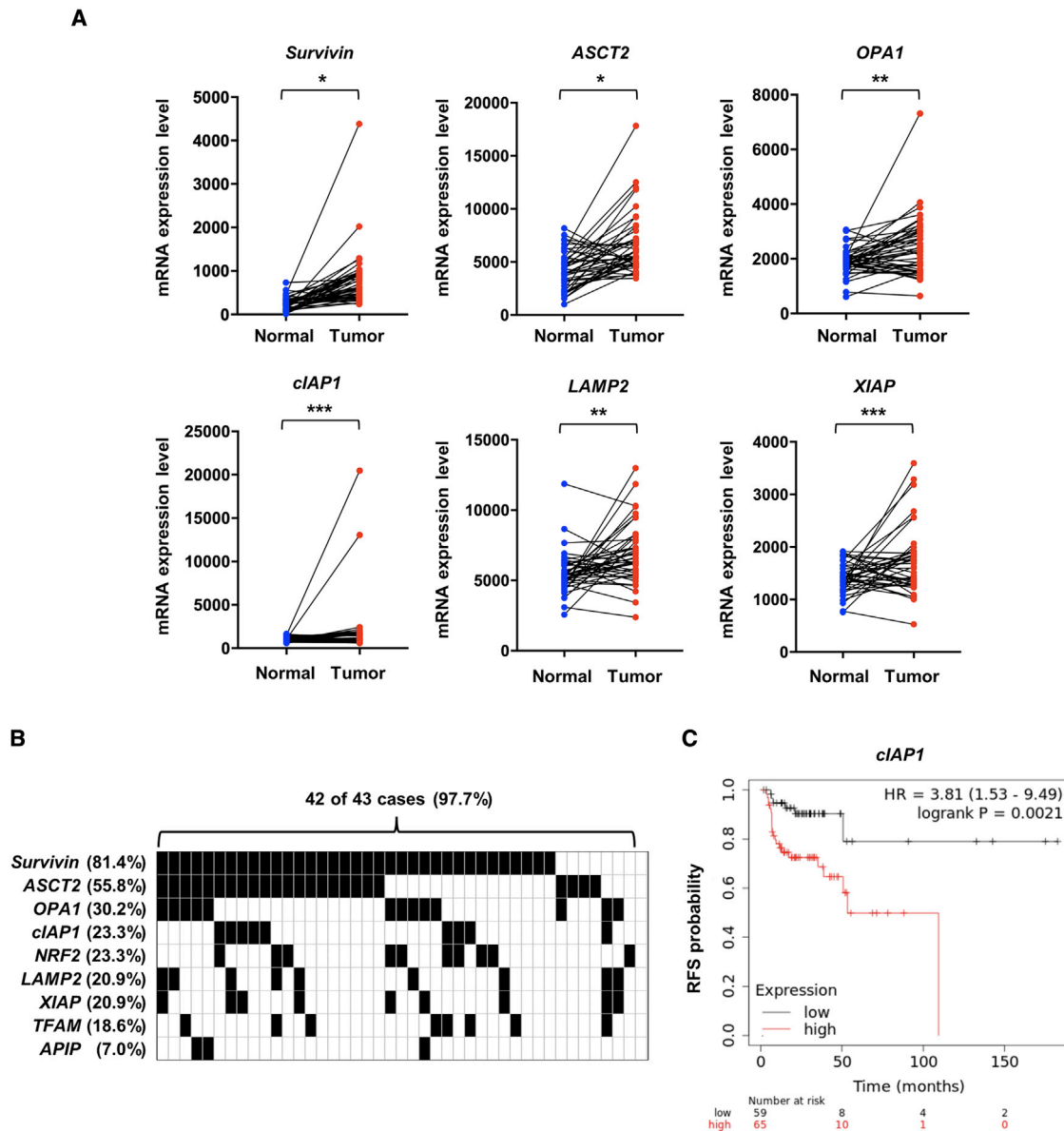


Figure 6. Upregulation of *miR-634* target genes in primary tumors

(A) Expression analysis in the 43 paired HNSCC samples of tumor tissue and corresponding adjacent non-tumor tissue for six target genes. p values were calculated using the paired Student's t test. * $p < 0.0001$, ** $p < 0.001$, and *** $p < 0.05$. (B) Summary of the expression status of *miR-634* target genes in 43 cases. Filled squares indicate the presence of cases with fold change (FC) more than 1.5, representing upregulation. (C) Kaplan-Meier survival curve of recurrence-free survival (RFS). p values were calculated using the log rank test ($p = 0.0021$).

normal tissue near the resection site.^{3,4,40} Furthermore, skin metastasis via infiltration of cancer cells is rarely observed, with an incidence ranging between 0.7% and 2.4%, especially in buccal mucosal carcinoma.^{41–43} Because topical treatment has the advantage of being able to be applied many times a day by the patient, *miR-634* ointment may be a minimally invasive topical medication for patients with a reduced quality of life due to bleeding and odoriferous exudates from skin infiltration.⁴⁴

Regarding miR therapeutics, there is a concern that “too many targets for miRNA effect” (TMTME) caused by the repression of multiple target genes may lead to unexpected adverse events.^{45,46} Indeed, a phase I study of the systemic administration of MRX34, a liposomal *miR-34a* mimic that can target multiple cancer-promoting genes, including *BCL2* and *PD-L1*, in patients with advanced solid tumors resulted in adverse immune responses.^{21,45} This adverse event was probably due to the repression of immune-related genes because *in*

silico miRNA target prediction, and pathway analysis revealed that *miR-34a* target genes include a number of immune-related genes.^{46,47} There is no association with immune-related systems in the *miR-634* target genes thus far; however, further validation of *miR-634* functions, including characterization of the other target genes, will be necessary for the clinical use of *miR-634* therapeutics. Furthermore, we noted the frequent upregulation of *miR-634* target genes in OSCC tumors. The high expression and gene amplification of *cIAP1* is closely associated with the recurrence of OSCC.^{48–50} Thus, dysregulated expression and genetic alteration of *miR-634* target genes may be useful biomarkers for stratifying patients who are expected to benefit from treatment with *miR-634* ointment. Further examinations, including expression analysis in large cohorts and investigations using a patient-derived xenograft (PDX) model, will lead to the practical application of *miR-634* ointment in clinical practice.

MATERIALS AND METHODS

Cell culture

OSCC cell lines were established from surgically resected tumors at the Tokyo Medical and Dental University (TMDU)⁵¹ or obtained from the Japanese Collection of Research Bioresources (JCRB) (Tokyo, Japan). The RT7 cell line was kindly provided by Dr. N. Kamata (Hiroshima University, Faculty of Dentistry, Japan).²⁹ T24 (bladder cancer cell line) was obtained from the JCRB. A2780 (ovarian cancer cell line) was kindly provided by Dr. Yong Sang Song (Seoul National University, Seoul, Korea).⁵² OSCC cell lines, T24, and A2780, were maintained in DMEM (WAKO, Tokyo, Japan) containing 10% FBS, 100 U/mL of penicillin, and 100 µg/mL of streptomycin. RT7 was maintained in KGM-2 Keratinocyte Growth Medium-2 BulletKit (Lonza, Basel, Switzerland). The cultures were maintained at 37°C with 5% CO₂. Cells were routinely checked for *Mycoplasma* contamination and cultured for no more than 20 passages from the validated stocks. Once resuscitated, the cell lines were authenticated by monitoring cell morphology.

Antibodies and reagents

Antibodies against the following proteins were used: cIAP1 (#7065), cCasp-3 (#9661), caspase-3 (#9662), cPARP (#9541), PARP (#9532), and Survivin (#2808) (Cell Signaling Technology, Danvers, MA, USA); TFAM (SAB1401383) (Sigma, St. Louis, MO, USA); OPA1 (ab42364) and LAMP2 (ab18529) (Abcam, Cambridge, UK); APIP (sc-376666) and β-actin (sc-69879) (Santa Cruz Biotechnology, Dallas, TX, USA); and XIAP (10037), NRF2 (16396), and ASCT2 (20350) (Proteintech, Rosemont, IL, USA). CDDP was purchased from Sigma.

Transfection of miRNA and siRNA

The *miRvana miR-634* mimic (4464066) and negative control 1 (*miR-NC*; 4464058) were purchased from Thermo Fisher Scientific (Waltham, MA, USA). siRNA for *cIAP1-1* (HSS100559) was from Thermo Fisher Scientific. The other siRNAs were synthesized by Sigma. Sequences for siRNAs are indicated in Table S4. Transfection was performed using Lipofectamine RNAiMAX (Invitrogen, Carlsbad, CA, USA) according to the manufacturer's instructions.²⁴

Cell survival assay

Cell survival was assessed by crystal violet (CV) staining as described in a previous paper.²⁴

Determination of the apoptotic cell population and intracellular ROS level by FACS analysis

The population of apoptotic cells was determined using the MEB-CYTO Apoptosis Kit (MBL, Nagoya, Japan). For the ROS detection assay, cells were incubated with 20 µM of DCFDA (dichlorodihydrofluorescein diacetate) for 30 min at 37°C with 5% CO₂. Fluorescence intensity in both procedures were measured using an Accuri Flow Cytometer (BD Biosciences, San Jose, CA, USA), as described in a previous paper.²⁴

In vivo tumor growth assay

All animal experiments were carried out according to the guidelines and approval by the TMDU Animal Care and Use Committee. Six-week-old female BALB/c nude mice were purchased from Charles River Laboratories (Yokohama, Japan). A total of 5.0×10^6 SAS cells in 100 µL of PBS were subcutaneously injected into the right flank of the mice. The 0.2% ointment incorporating ds-*miR-NC* mimic or ds-*miR-634* mimic was formulated (2 mg miRNA/mL ointment) using ILTS (MEDRx, Kagawa, Japan).²⁴ The ointment (10–20 µL; 20–40 µg of miRNA) was topically applied every other day onto subcutaneous tumors. CDDP was administered by IP injection at 4 mg/kg, two times per week.

Generation of CDDP-resistant cells

CDDP-resistant cells from Ca9-22 were generated by long-term cultivation in gradually increasing CDDP concentrations, as described in a previous paper.²³ The cells were initially exposed to CDDP at a low concentration (0.5 µmol/L) for three days, cultured in CDDP-free medium to confluence, and then exposed to CDDP at a higher concentration; this cycle was repeated five times with gradually increasing concentrations (0.5 µmol/L, 1 µmol/L, 2 µmol/L, 4 µmol/L, and 10 µmol/L of CDDP). The cells that survived in 10 µmol/L of CDDP were defined as CDDP-resistant cells (Ca9-22-R).

Immunohistochemistry (IHC)

Immunohistochemistry (IHC) analysis using section slides from xenograft tumors was performed as described in a previous paper.²⁴

qRT-PCR and genomic PCR

qRT-PCR was performed using TaqMan MicroRNA Assays (*miR-634*; assay ID: 001576; *RNU6B*; assay ID: 001093) (Applied Biosystems, Waltham, MA, USA), as described in a previous paper.²⁴ For genomic PCR, genomic DNA from RT7 cells was used as the control to measure the relative DNA copy number. Primer sequences are indicated in Table S4.

Western blotting

Western blotting was performed as described in a previous paper.²⁴ The bound antibodies were visualized with a LAS-3000 imaging

system (Fujifilm, Tokyo, Japan) using a Pierce ECL western blot detection kit (Thermo Scientific).

RIP-Chip and RIP-PCR analyses

RIP was performed according to the manufacturer's instructions for the RiboCluster Profiler RIP-Assay Kit for miRNA (MBL), as described in a previous paper.²⁴ Expression array analysis using RNA from AGO2-RIP and total RNA (input) was performed on the Agilent 8 × 60K array and GeneSpring software, according to the manufacturer's instructions (Agilent Technologies, Santa Clara, CA, USA). The microarray data in SAS cells have been submitted to the Gene Expression Omnibus (GEO) database (<http://www.ncbi.nlm.nih.gov/geo/>) and assigned the identifier GSE194269. Data (GSE159093) for RIP-Chip analysis in A431 cells were used. For RIP-PCR analysis, cDNA was synthesized from RNA isolated by AGO2-RIP or IgG-RIP and from total RNA (input), and qRT-PCR was performed. Primer sequences are indicated in [Table S4](#).

KEGG pathway analysis

The KEGG pathway analysis was conducted using DAVID (<https://david.ncifcrf.gov/summary.jsp>), and an enrichment score with $p < 0.05$ was considered significant.⁵³

Combination index (CI)

Cells were treated with the indicated therapeutic combinations, and cell viability was measured using a CV staining assay. The CI was calculated using CalcuSyn (Biosoft, Cambridge, UK). CI <1 indicates a synergistic drug–drug interaction.

Analysis of the public expression data

Expression data for tumor and non-tumor tissue in 43 paired samples of primary HNSCC from The Cancer Genome Atlas (TCGA) project were used. The frequencies of genes highly expressed in tumor tissues relative to the corresponding non-tumor tissue were calculated. For correlation analysis in 496 cases of HNSCC, including OSCC, a log₂ transformation was applied to the expression values and copy number values, and the dot plot for the correlation were generated on the cBioPortal website (<https://www.cbioportal.org>). Kaplan-Meier survival curves of RFS and OS were generated on the Kaplan-Meier plotter database.⁵⁴

Luciferase reporter assay

The luciferase assay was performed as described in a previous paper.²⁰ Each PCR product corresponding to two putative *miR-634* binding sites (S1 and S2) within the *cIAP1* gene was inserted into the pmir-GLO Dual-Luciferase miRNA Target Expression Vector (Promega, WI, USA). Site-specific mutagenesis was performed using the KOD-Plus- mutagenesis kit (Toyobo, Osaka, Japan). The luciferase activity was measured using the dual-luciferase reporter assay system (Promega). Primer sequences used in this assay are indicated in [Table S4](#).

Statistical analysis

Significance was assessed by the two-tailed Student's *t* test or ANOVA (for multiple comparisons) using Prism version 5.04 (GraphPad, La

Jolla, CA). Results with $p \leq 0.05$ were considered significant. For correlation analysis, the Pearson scores and *p* value were computed on the cBioPortal. The Kaplan-Meier plotter was used to calculate the hazard ratio (HR) and its corresponding 95% confidence interval (95% CI).⁵⁴ The significance of effects of gene expression levels on patient survival was assessed by the log rank test.

SUPPLEMENTAL INFORMATION

Supplemental information can be found online at <https://doi.org/10.1016/j.omto.2022.02.002>.

ACKNOWLEDGMENTS

We would like to thank Dr. Masahiko Miura and Dr. Hitomi Nojima (Department of Oral Radiation Oncology, TMDU) for discussion regarding this manuscript, Dr. Yong Sang Song (Seoul National University, Seoul, Korea) for providing the cell line, and Ayako Takahashi and Rumi Mori (TMDU) for their technical assistance. This work was supported in part by Grants-in-Aid for Scientific Research (21H02781 to J. Inoue and 18H02688 to J. Inazawa), a Grant-in-Aid for Scientific Research on Innovative Areas “Conquering cancer through NEO-dimensional systems understandings” (15H05908 to J. Inazawa) from JSPS and MEXT, a research program of the Project for Cancer Research and Therapeutic Evolution (P-CREATE), and the Tailor-Made Medical Treatment with the BioBank Japan Project (BBJ) from the Japan Agency for Medical Research and Development (AMED). This study was supported by Nanken-Kyoten, TMDU.

AUTHOR CONTRIBUTIONS

P.X.T., Ju.I., and J.I. contributed to the conception and design of study. P.X.T. and Ju.I. contributed to the acquisition and interpretation of data. H.H. provided information for clinical implication. P.X.T., Ju.I., and J.I. wrote the manuscript.

DECLARATION OF INTERESTS

The authors declare no conflicts of interest.

REFERENCES

- Colevas, A.D., Yom, S.S., Pfister, D.G., Spencer, S., Adelstein, D., Adkins, D., Brizel, D.M., Burtneess, B., Busse, P.M., Caudell, J.J., et al. (2018). NCCN guidelines insights: head and neck cancers, version 1. *J. Natl. Compr. Canc Netw.* *16*, 479–490.
- Bray, F., Ferlay, J., Soerjomataram, I., Siegel, R.L., Torre, L.A., and Jemal, A. (2018). Global cancer statistics 2018: GLOBOCAN estimates of incidence and mortality worldwide for 36 cancers in 185 countries. *CA Cancer J. Clin.* *68*, 394–424.
- Bloebaum, M., Poort, L., Böckmann, R., and Kessler, P. (2014). Survival after curative surgical treatment for primary oral squamous cell carcinoma. *J. Craniomaxillofac. Surg.* *42*, 1572–1576.
- Cramer, J.D., Burtneess, B., Le, Q.T., and Ferris, R.L. (2019). The changing therapeutic landscape of head and neck cancer. *Nat. Rev. Clin. Oncol.* *16*, 669–683.
- Johnson, D.E., Burtneess, B., Leemans, C.R., Lui, V.W.Y., Bauman, J.E., and Grandis, J.R. (2020). Head and neck squamous cell carcinoma. *Nat. Rev. Dis. Primers* *6*, 92.
- Rottenberg, S., Disler, C., and Perego, P. (2021). The rediscovery of platinum-based cancer therapy. *Nat. Rev. Cancer* *21*, 37–50.
- Kernohan, M.D., Clark, J.R., Gao, K., Ebrahimi, A., and Milross, C.G. (2010). Predicting the prognosis of oral squamous cell carcinoma after first recurrence. *Arch. Otolaryngol. Head Neck Surg.* *136*, 1235–1239.

8. Vucic, D. (2008). Targeting IAP (inhibitor of apoptosis) proteins for therapeutic intervention in tumors. *Curr. Cancer Drug Targets* 8, 110–117.
9. Cancer Genome Atlas Network (2015). Comprehensive genomic characterization of head and neck squamous cell carcinomas. *Nature* 517, 576–582.
10. Imoto, I., Yang, Z.Q., Pimkhaokham, A., Tsuda, H., Shimada, Y., Imamura, M., Ohki, M., and Inazawa, J. (2001). Identification of cIAP1 as a candidate target gene within an amplicon at 11q22 in esophageal squamous cell carcinomas. *Cancer Res.* 61, 6629–6634.
11. Imoto, I., Tsuda, H., Hirasawa, A., Miura, M., Sakamoto, M., Hirohashi, S., and Inazawa, J. (2002). Expression of cIAP1, a target for 11q22 amplification, correlates with resistance of cervical cancers to radiotherapy. *Cancer Res.* 62, 4860–4866.
12. Cai, Q., Sun, H., Peng, Y., Lu, J., Nikolovska-Coleska, Z., McEachern, D., Liu, L., Qiu, S., Yang, C.Y., Miller, R., et al. (2011). A potent and orally active antagonist (SM-406/AT-406) of multiple inhibitor of apoptosis proteins (IAPs) in clinical development for cancer treatment. *J. Med. Chem.* 54, 2714–2726.
13. Matzinger, O., Viertl, D., Tsoutsou, P., Kadi, L., Rigotti, S., Zanna, C., Wiedemann, N., Vozenin, M.C., Vuagniaux, G., and Bourhis, J. (2015). The radiosensitizing activity of the SMAC-mimetic, Debio 1143, is TNF α -mediated in head and neck squamous cell carcinoma. *Radiother. Oncol.* 116, 495–503.
14. Thibault, B., Genre, L., Le Naour, A., Broca, C., Mery, E., Vuagniaux, G., Delord, J.P., Wiedemann, N., and Couderc, B. (2018). DEBIO 1143, an IAP inhibitor, reverses carboplatin resistance in ovarian cancer cells and triggers apoptotic or necroptotic cell death. *Sci. Rep.* 8, 17862.
15. Le Tourneau, C., Tao, Y., Gomez-Roca, C., Cristina, V., Borcoman, E., Deutsch, E., Bahleda, R., Calugaru, V., Modesto, A., Rouits, E., et al. (2020). Phase I trial of Debio 1143, an antagonist of inhibitor of apoptosis proteins, combined with cisplatin chemoradiotherapy in patients with locally advanced squamous cell carcinoma of the head and neck. *Clin. Cancer Res.* 26, 6429–6436.
16. Sun, X.S., Tao, Y., Le Tourneau, C., Pointreau, Y., Sire, C., Kaminsky, M.C., Coutte, A., Alfonsi, M., Boisselier, P., Martin, L., et al. (2020). Debio 1143 and high-dose cisplatin chemoradiotherapy in high-risk locoregionally advanced squamous cell carcinoma of the head and neck: a double-blind, multicentre, randomised, phase 2 study. *Lancet Oncol.* 21, 1173–1187.
17. Gomez-Roca, C., Delord, J.P., Even, C., Basté, N., Temam, S., Le Tourneau, C., Hoffmann, C., Borcoman, E., Sarini, J., Vergez, S., et al. (2021). Exploratory window-of-opportunity trial to investigate the tumor pharmacokinetics/pharmacodynamics of the IAP antagonist Debio 1143 in patients with head and neck cancer. *Clin. Transl. Sci.* 15, 55–62.
18. Gebert, L.F.R., and MacRae, I.J. (2019). Regulation of microRNA function in animals. *Nat. Rev. Mol. Cell Biol.* 20, 21–37.
19. Inoue, J., and Inazawa, J. (2021). Cancer-associated miRNAs and their therapeutic potential. *J. Hum. Genet.* 66, 937–945.
20. Kozaki, K., and Inazawa, J. (2012). Tumor-suppressive microRNA silenced by tumor-specific DNA hypermethylation in cancer cells. *Cancer Sci.* 103, 837–845.
21. Winkle, M., El-Daly, S.M., Fabbri, M., and Calin, G.A. (2021). Noncoding RNA therapeutics -challenges and potential solutions. *Nat. Rev. Drug Discov.* 20, 629–651.
22. Yamamoto, S., Inoue, J., Kawano, T., Kozaki, K., Omura, K., and Inazawa, J. (2014). The impact of miRNA-based molecular diagnostics and treatment of NRF2-stabilized tumors. *Mol. Cancer Res.* 12, 58–68.
23. Fujiwara, N., Inoue, J., Kawano, T., Tanimoto, K., Kozaki, K., and Inazawa, J. (2015). miR-634 activates the mitochondrial apoptosis pathway and enhances chemotherapy-induced cytotoxicity. *Cancer Res.* 75, 3890–3901.
24. Inoue, J., Fujiwara, K., Hamamoto, H., Kobayashi, K., and Inazawa, J. (2020). Improving the efficacy of EGFR inhibitors by topical treatment of cutaneous squamous cell carcinoma with miR-634 ointment. *Mol. Ther. Oncolytics* 19, 294–307.
25. Gokita, K., Inoue, J., Ishihara, H., Kojima, K., and Inazawa, J. (2020). Therapeutic potential of LNP-mediated delivery of miR-634 for cancer therapy. *Mol. Ther. Nucleic Acids* 19, 330–338.
26. Kishikawa, M., Inoue, J., Hamamoto, H., Kobayashi, K., Asakage, T., and Inazawa, J. (2021). Augmentation of lenvatinib efficacy by topical treatment of miR-634 ointment in anaplastic thyroid cancer. *Biochem. Biophys. Rep.* 26, 101009.
27. Kobayashi, H., and Tomari, Y. (2016). RISC assembly: coordination between small RNAs and Argonaute proteins. *Biochim. Biophys. Acta* 1859, 71–81.
28. Keene, J.D., Komisarow, J.M., and Friedersdorf, M.B. (2006). RIP-Chip: the isolation and identification of mRNAs, microRNAs and protein components of ribonucleo-protein complexes from cell extracts. *Nat. Protoc.* 1, 302–307.
29. Fujimoto, R., Kamata, N., Yokoyama, K., Taki, M., Tomonari, M., Tsutsumi, S., Yamanouchi, H., Tomonari, M., and Nagayama, M. (2002). Establishment of immortalized human oral keratinocytes by gene transfer of a telomerase component. *J. Jpn. Oral Muco Membr.* 8, 1–8.
30. Saleem, M., Qadir, M.I., Perveen, N., Ahmad, B., Saleem, U., Irshad, T., and Ahmad, B. (2013). Inhibitors of apoptotic proteins: new targets for anticancer therapy. *Chem. Biol. Drug Des.* 82, 243–251.
31. Cho, D.H., Hong, Y.M., Lee, H.J., Woo, H.N., Pyo, J.O., Mak, T.W., and Jung, Y.K. (2004). Induced inhibition of ischemic/hypoxic injury by APIP, a novel Apaf-1-interacting protein. *J. Biol. Chem.* 279, 39942–39950.
32. Mirzaei, S., Hushmandi, K., Zabolian, A., Saleki, H., Torabi, S.M.R., Ranjbar, A., SeyedSaleh, S., Sharifzadeh, S.O., Khan, H., Ashrafzadeh, M., et al. (2021). Elucidating role of reactive oxygen species (ROS) in cisplatin chemotherapy: a focus on molecular pathways and possible therapeutic strategies. *Molecules* 26, 2382.
33. Mirzaei, S., Mohammadi, A.T., Gholami, M.H., Hashemi, F., Zarrabi, A., Zabolian, A., Hushmandi, K., Makvandi, P., Samec, M., Liskova, A., et al. (2021). Nrf2 signaling pathway in cisplatin chemotherapy: potential involvement in organ protection and chemoresistance. *Pharmacol. Res.* 167, 105575.
34. Wang, C., Wu, J., Wang, Z., Yang, Z., Li, Z., Deng, H., Li, L., Peng, X., and Feng, M. (2018). Glutamine addiction activates polyglutamine-based nanocarriers delivering therapeutic siRNAs to orthotopic lung tumor mediated by glutamine transporter SLC1A5. *Biomaterials* 183, 77–92.
35. Fang, H.Y., Chen, C.Y., Chiou, S.H., Wang, Y.T., Lin, T.Y., Chang, H.W., Chiang, I.P., Lan, K.J., and Chow, K.C. (2012). Overexpression of optic atrophy 1 protein increases cisplatin resistance via inactivation of caspase-dependent apoptosis in lung adenocarcinoma cells. *Hum. Pathol.* 43, 105–114.
36. Xie, D., Wu, X., Lan, L., Shangguan, F., Lin, X., Chen, F., Xu, S., Zhang, Y., Chen, Z., Huang, K., et al. (2016). Downregulation of TFAM inhibits the tumorigenesis of non-small cell lung cancer by activating ROS-mediated JNK/p38MAPK signaling and reducing cellular bioenergetics. *Oncotarget* 7, 11609–11624.
37. González-Polo, R.A., Boya, P., Pauleau, A.L., Jalil, A., Larochette, N., Souquère, S., Eskelinen, E.L., Pierron, G., Saftig, P., and Kroemer, G. (2005). The apoptosis/autophagy paradox: autophagic vacuolization before apoptotic death. *J. Cell Sci.* 118, 3091–3102.
38. Miwa, Y., Hamamoto, H., and Ishida, T. (2016). Lidocaine self-sacrificially improves the skin permeation of the acidic and poorly water-soluble drug etodolac via its transformation into an ionic liquid. *Eur. J. Pharm. Biopharm.* 102, 92–100.
39. Kubota, K., Shibata, A., and Yamaguchi, T. (2016). The molecular assembly of the ionic liquid/aliphatic carboxylic acid/aliphatic amine as effective and safety transdermal permeation enhancers. *Eur. J. Pharm. Sci.* 86, 75–83.
40. Huang, S.H., and O'Sullivan, B. (2013). Oral cancer: current role of radiotherapy and chemotherapy. *Med. Oral Patol Oral Cir Bucal.* 18, e233–e240.
41. Pitman, K.T., and Johnson, J.T. (1999). Skin metastases from head and neck squamous cell carcinoma: incidence and impact. *Head Neck* 21, 560–565.
42. Yuskovitch, A., Hier, M.P., Okrainec, A., Black, M.J., and Rochon, L. (2001). Skin metastases in squamous cell carcinoma of the head and neck. *Otolaryngol. Head Neck Surg.* 124, 248–252.
43. Srinivasan, S., Leekha, N., Gupta, S., Mithal, U., Arora, V., and De, S. (2016). Distant skin metastases from carcinoma buccal mucosa: a rare presentation. *Indian J. Dermatol.* 61, 468.
44. Kakimoto, M., Tokita, H., Okamura, T., and Yoshino, K. (2010). A chemical hemostatic technique for bleeding from malignant wounds. *J. Palliat. Med.* 13, 11–13.
45. Hong, D.S., Kang, Y.K., Borad, M., Sachdev, J., Ejadi, S., Lim, H.Y., Brenner, A.J., Park, K., Lee, J.L., Kim, T.Y., et al. (2020). Phase 1 study of MRX34, a liposomal miR-34a mimic, in patients with advanced solid tumours. *Br. J. Cancer* 122, 1630–1637.

46. Zhang, S., Cheng, Z., Wang, Y., and Han, T. (2021). The risks of miRNA therapeutics: in a drug target perspective. *Drug Des. Devel Ther.* 15, 721–733.
47. Hart, M., Nickl, L., Walch-Rueckheim, B., Krammes, L., Rheinheimer, S., Diener, C., Taenzer, T., Kehl, T., Sester, M., Lenhof, H.P., et al. (2020). Wrinkle in the plan: miR-34a-5p impacts chemokine signaling by modulating CXCL10/CXCL11/CXCR3-axis in CD4⁺, CD8⁺ T cells, and M1 macrophages. *J. Immunother. Cancer* 8, e001617.
48. Tanimoto, T., Tsuda, H., Imazeki, N., Ohno, Y., Imoto, I., Inazawa, J., and Matsubara, O. (2005). Nuclear expression of cIAP-1, an apoptosis inhibiting protein, predicts lymph node metastasis and poor patient prognosis in head and neck squamous cell carcinomas. *Cancer Lett.* 224, 141–151.
49. Qi, S., Mogi, S., Tsuda, H., Tanaka, Y., Kozaki, K., Imoto, I., Inazawa, J., Hasegawa, S., and Omura, K. (2008). Expression of cIAP-1 correlates with nodal metastasis in squamous cell carcinoma of the tongue. *Int. J. Oral Maxillofac. Surg.* 37, 1047–1053.
50. Bhosale, P.G., Pandey, M., Cristea, S., Shah, M., Patil, A., Beerwinkler, N., Schäffer, A.A., and Mahimkar, M.B. (2017). Recurring amplification at 11q22.1-q22.2 locus plays an important role in lymph node metastasis and radioresistance in OSCC. *Sci. Rep.* 7, 16051.
51. Akanuma, D., Uzawa, N., Yoshida, M.A., Negishi, A., Amagasa, T., and Ikeuchi, T. (1999). Inactivation patterns of the p16 (INK4a) gene in oral squamous cell carcinoma cell lines. *Oral Oncol.* 35, 476–483.
52. Furusawa, A., Miyamoto, M., Takano, M., Tsuda, H., Song, Y.S., Aoki, D., Miyasaka, N., Inazawa, J., and Inoue, J. (2018). Ovarian cancer therapeutic potential of glutamine depletion based on GS expression. *Carcinogenesis* 39, 758–766.
53. Kanehisa, M., and Goto, S. (2000). KEGG: kyoto encyclopedia of genes and genomes. *Nucleic Acids Res.* 28, 27–30.
54. Györfy, B., Lanczky, A., Eklund, A.C., Denkert, C., Budczies, J., Li, Q., and Szallasi, Z. (2010). An online survival analysis tool to rapidly assess the effect of 22,277 genes on breast cancer prognosis using microarray data of 1,809 patients. *Breast Cancer Res. Treat* 123, 725–731.